Understanding paramagnetic spin correlations in the spin-liquid pyrochlore Tb$_2$Ti$_2$O$_7$

Ying-Jer Kao,[1,2,*] Matthew Enjalran,[1,3] Adrian Del Maestro,[1,4] Hamid R. Molavian,[1] and Michel J. P. Gingras[1,5]

[1]*Department of Physics, University of Waterloo, Waterloo, Ontario, Canada N2L 3G1*

[2]*Department of Physics, University of Toronto, Toronto, Ontario, Canada M5S 1A7*

[3]*Department of Physics, Southern Connecticut State University, New Haven, Connecticut 06515, USA*

[4]*Department of Physics, Yale University, New Haven, Connecticut 06520, USA*

[5]*Canadian Institute for Advanced Research, Toronto, Ontario, Canada M5G 1Z8*

Recent elastic and inelastic neutron scattering studies of the highly frustrated pyrochlore antiferromagnet Tb$_2$Ti$_2$O$_7$ have shown some very intriguing features that cannot be modeled by the local $\langle 111 \rangle$ classical Ising model, naively expected to describe this system at low temperatures. By including single-ion excitations from the ground state doublet to higher crystal field levels, we successfully describe the elastic neutron scattering pattern and dispersion relations in Tb$_2$Ti$_2$O$_7$, quantitatively consistent with experimental observations.

The search for the physical realization of a spin liquid in three dimensions has been a long quest for the condensed matter community. Recently, geometrically frustrated magnetic systems have been the focus of intensive experimental and theoretical studies because it is believed that geometrical frustration can inhibit the formation of long-range order, thus enabling the system to remain paramagnetic down to low temperatures. Among three-dimensional systems, the pyrochlore lattice of corner-sharing tetrahedra have been studied extensively. It has been shown theoretically and numerically[1–3] that for classical Heisenberg spins with nearest-neighbor antiferromagnetic (AF) exchange, there is no transition to long-range magnetic order at finite temperature. This makes AF materials based on the pyrochlore lattice excellent candidates to search for the low-temperature spin-liquid state. A number of experimental studies on insulating pyrochlore materials have been carried out. Interestingly, most materials either develop long-range Néel order, such as Gd$_2$Ti$_2$O$_7$ (Ref. 4) and Er$_2$Ti$_2$O$_7$,[5] or reveal spin-glass behavior, such as Y$_2$Mo$_2$O$_7$.[6] The "spin-ice" materials, Ho$_2$Ti$_2$O$_7$[7,8] and Dy$_2$Ti$_2$O$_7$[9,10] exhibit low-temperature thermodynamic properties reminiscent of Pauling's "water ice model."[11] In these systems, an effective ferromagnetic interaction is frustrated due to the single-ion $\langle 111 \rangle$ Ising anisotropy.[11,12] The behavior of these systems can be quantitatively described by the $\langle 111 \rangle$ Ising spin model with nearest-neighbor exchange and long-range dipolar interactions.[8,10,11]

Tb$_2$Ti$_2$O$_7$ shows, however, very different and intriguing behavior. It is believed that Tb$_2$Ti$_2$O$_7$ belongs to the same family of $\langle 111 \rangle$ Ising systems as Dy$_2$Ti$_2$O$_7$ and Ho$_2$Ti$_2$O$_7$ but with an effective nearest neighbor AF interaction.[10,13–16] The same spin model that very successfully describes the spin-ice systems predicts it to have a noncollinear Néel **Q** $=0$ order, with all spins pointing into or out of each tetrahedron, at about 1 K.[10] In dramatic contrast, Tb$_2$Ti$_2$O$_7$ remains a spin liquid, or "cooperative paramagnet," down to 70 mK.[13,16] In addition, recent paramagnetic neutron scattering studies show that the scattering pattern for this material is not consistent with a $\langle 111 \rangle$ Ising model, while a Heisenberg spin model[16,17] or some level of relaxation away from the

$\langle 111 \rangle$ Ising model[18] can better describe the observed neutron scattering pattern. These results suggest that the restoration of spin isotropy in the system, despite its expected Ising-like nature at low temperature,[14,19–21] is essential in understanding the paramagnetic spin correlations. Inelastic neutron scattering studies have also been performed on this system and partial softening of the magnetic excitations at an energy of about 20 K has been observed.[13,16,22] This has been attributed to a (spin) roton-like mode, as in liquid ^{4}He,[13,16,23] which further indicates a more isotropic nature of the spins. Given the ensemble of evidences, it would appear that one needs a more isotropic spin model to understand the paramagnetic spin correlations in this system. More importantly, such a "restoration" of spin isotropy may also be the key to understanding why Tb$_2$Ti$_2$O$_7$ fails to order down to low temperatures. In this paper, we employ the random-phase approximation (RPA)[24] to take into account the single-ion excitations from the ground-state doublet to the first excited doublet. We successfully describe the observed paramagnetic spin correlations in Tb$_2$Ti$_2$O$_7$, without any assumptions regarding the nature of the spins, while we still obtain the **Q** $=0$ Néel order at low temperatures. This result makes the fact that Tb$_2$Ti$_2$O$_7$ fails to order even more puzzling.

We begin with the model spin Hamiltonian,

$$\mathcal{H} = \frac{1}{2} \sum_{i,j,\alpha,\beta,a,b} J_{i,a}^{\alpha} \mathcal{J}_{ab}^{\alpha\beta}(i,j) J_{j,b}^{\beta} + \sum_{i,a} \mathcal{H}_{\mathrm{CF}}(i,a), \quad (1)$$

where i,j are indices of the Bravais lattice vectors for the fcc lattice, a,b are indices of the sublattice basis vectors, and α,β are indices for the spatial coordinates. $\mathcal{H}_{\mathrm{CF}}$ is the single-ion crystal field (CF) Hamiltonian. The spin-spin interaction matrix $\mathcal{J}$, including both exchange and long-range dipolar interactions, reads

$$\mathcal{J}_{ab}^{\alpha\beta}(i,j) = -\mathcal{J}_1 \delta^{\alpha\beta} \delta_{nn} + D_{dd} \left[\frac{\delta^{\alpha\beta}}{|\mathbf{R}_{ij}^{ab}|^3} - \frac{3 R_{ij}^{ab,\alpha} R_{ij}^{ab,\beta}}{|\mathbf{R}_{ij}^{ab}|^5} \right],$$

where δ_{nn} refers to nearest-neighbor interaction, and $R_{ij}^{ab,\alpha}$ denotes the α component of the interspin vector $\mathbf{R}_{ij}^{ab}$ that connects spins $\mathbf{J}_{i,a}$ and $\mathbf{J}_{j,b}$. The nearest-neighbor exchange

for $Tb_2Ti_2O_7$ is given by $\mathcal{J}_1 \approx -0.167$ K,[25] and $D_{dd} = (g\mu_B)^2 \mu_0/4\pi$, where μ_B is the Bohr magneton, μ_0 is the magnetic permeability, and $g = 3/2$ for Tb^{3+}.

The single-ion susceptibility is given by[24]

$$\chi_a^{0,\alpha\beta}(\omega) = \sum_{\mu,\nu}^{E_\mu \neq E_\nu} \frac{M_{\nu\mu,a}^\alpha M_{\mu\nu,a}^\beta}{E_\mu - E_\nu - \hbar(\omega + i0^+)}(n_\nu - n_\mu)$$
$$+ \frac{\delta(\omega)}{k_B T} \sum_{\mu,\nu}^{E_\mu = E_\nu} M_{\nu\mu,a}^\alpha M_{\mu\nu,a}^\beta n_\nu, \quad (2)$$

where n_ν is the thermal occupation fraction for state ν. The matrix elements for the single-ion states are given by $M_{\nu\mu,a}^\alpha = \Sigma_{\bar{\alpha}}\langle \nu|J^{\bar{\alpha}}|\mu\rangle u_{\bar{\alpha},a}^\alpha$, where $u_{\bar{\alpha},a}^\alpha$ is the rotation matrix from the local ($\bar{\alpha}$) frame defined on sublattice a to the global (α) frame. The angular momentum operator $J^{\bar{\alpha}}$ acts on the CF states defined along the local quantization axis.[14] The local wave function structure has been obtained from both experimental measurements and theoretical calculations.[14,20,21] The primary components are J_z eigenstates $|\pm 4\rangle$ for the ground state doublet and $|\pm 5\rangle$ for the first-excited state doublet. There are finite J^+ or J^- matrix elements between the two doublets that are separated by an anisotropy gap $\Delta \approx 20$ K, which is comparable with the Curie-Weiss temperature $\theta_{CW} \approx -19$ K.[14] With this Ising-like wave function, our model reduces to a $\langle 111 \rangle$ Ising model at low temperatures, while allowing excitations to the excited states.

The RPA equation which takes into account the two-ion interaction contribution to the full susceptibility[24] is given by

$$\chi_{ab}^{\alpha\beta}(\mathbf{q},\omega) + \sum_{\gamma,\delta,c} \chi_a^{0,\alpha\gamma}(\omega)\mathcal{J}_{ac}^{\gamma\delta}(\mathbf{q})\chi_{cb}^{\delta\beta}(\mathbf{q},\omega) = \delta_{ab}\chi_a^{0,\alpha\beta}(\omega),$$

where $\mathcal{J}(\mathbf{q})$ is the Fourier transformation of the interaction matrix $\mathcal{J}(i,j)$. The slowly converging, infinite lattice sum of the dipolar interaction is handled using Ewald summation techniques.[17,26] We solve for $\chi_{ab}^{\alpha\beta}(\mathbf{q},\omega)$ numerically using LAPACK routines.

The elastic and dynamical neutron cross sections are related to the spin susceptibilities by summing over the sublattice contributions and taking the transverse components of $\mathbf{J}$ perpendicular to $\mathbf{Q}$,[24]

$$S_{el}(\mathbf{Q}) \propto \frac{|F(\mathbf{Q})|^2}{k_B T} \sum_{\alpha,\beta;a,b} (\delta_{\alpha\beta} - \hat{Q}_\alpha \hat{Q}_\beta)$$
$$\times \exp[-i(\mathbf{r}^a - \mathbf{r}^b)\cdot\mathbf{G}]\mathrm{Re}\,\chi_{ab}^{\alpha\beta}(\mathbf{q}), \quad (3a)$$

$$S_{dyn}(\mathbf{Q},\omega) \propto \frac{|F(\mathbf{Q})|^2}{1 - \exp(-\hbar\omega/k_B T)} \sum_{\alpha,\beta;a,b} (\delta_{\alpha\beta} - \hat{Q}_\alpha \hat{Q}_\beta)$$
$$\times \exp[-i(\mathbf{r}^a - \mathbf{r}^b)\cdot\mathbf{G}]\mathrm{Im}\,\chi_{ab}^{\alpha\beta}(\mathbf{q},\omega), \quad (3b)$$

where $\mathbf{Q} = \mathbf{G} + \mathbf{q}$, $\mathbf{G}$ is a reciprocal lattice vector of the fcc lattice, and $\mathbf{q}$ is a primitive vector in the first Brillouin zone. $\mathbf{r}^a$ is the sublattice basis vector and $F(\mathbf{Q})$ is the magnetic form factor for Tb^{3+}.

Figure 1(a) shows the experimental scattering pattern in the (h,h,l) plane at 9 K.[16] Note that there is a strong intensity maximum around (0,0,2). Figure 1(b) shows the $S(\mathbf{Q})$ calculation using the $\langle 111 \rangle$ Ising model, i.e., the anisotropy gap $\Delta \to \infty$. It is clear that this model fails to reproduce the correct neutron scattering pattern as observed experimentally, as there is only weak noncritical intensity around (0,0,2). It has been shown that in the $\langle 111 \rangle$ Ising model, the intensity at (0,0,2) and (0,0,0) are exactly correlated, and vanishes for $Tb_2Ti_2O_7$.[14,16,17] Using a more realistic doublet-doublet model for $Tb_2Ti_2O_7$, we are able to qualitatively reproduce the experimentally observed scattering pattern [Fig. 1(c)]. It captures most details of the experimental pattern, such as the intensity maximum around (0,0,2), the minima around (0,0,0), (2,2,2), and (0,0,4). This excellent agreement between theory and experiment indicates that to properly understand the spin correlations in $Tb_2Ti_2O_7$, the excitations out of the ground state doublet to the first excited doublet, originating from the first term in Eq. (2), are important. It should be noted that this result is obtained from the simple level scheme described above with no other assumptions about the nature of the spin or the details of the wave functions.

Line scans in reciprocal space along three high-symmetry directions $(0,0,l)$, $(h,h,0)$, and (h,h,h) at $T = 4$ K are plotted in Fig. 2. Open symbols are the data points for $S(\mathbf{Q})$. Filled symbols are the dispersion relations $E(\mathbf{Q})$ for the lowest-energy band of magnetic excitations at 4 K. The dispersion relations show good quantitative agreement with the experimental dispersion observed in single crystal $Tb_2Ti_2O_7$ reported in Fig. 9 of Ref. 16. We also find that the minimum in $E(\mathbf{Q})$ corresponds to the maximum in $S(\mathbf{Q})$ in all symmetry directions, as is observed in the experiment. The sharp jumps in dispersions, e.g., near (0,0,1) and (0,0,3), correspond to shifts of spectral maximum between different branches, since the experiment and current calculation track only the maximum peaks in the energy spectra. In principle, there should be four branches of magnetic excitations with different intensities due to the four sublattice structure. Higher resolution experiments need to be performed to map out the dispersion relations of these branches.

To study the temperature effects on the dispersion relations of the lowest three bands of magnetic excitations, we use the wave functions obtained from crystal field calculations in the point charge approximation and in the fixed $J = 6$ manifold for Tb^{3+}.[14] This gives the CF level scheme with two low-lying doublets as described above, and two higher-energy singlets.[14,16] The energy levels are given as 0, 24.6, 113.9, and 132.7 K, consistent with experiments. The two higher singlets have large $|\pm 3\rangle$ contributions and some mixing with other $|J, M_J\rangle$ components.[14] All the excited states are connected to the ground-state doublet through the J^+ and J^- operations and the excitations are visible via neutron spectroscopy.[16] Figure 3 shows the dispersion relations of the three lowest-lying magnetic excitations along (h,h,h) at 12 K and 30 K at the same energy scale. The lowest band becomes more dispersive as the temperature is lowered, while the higher two bands do not show much change with temperature.
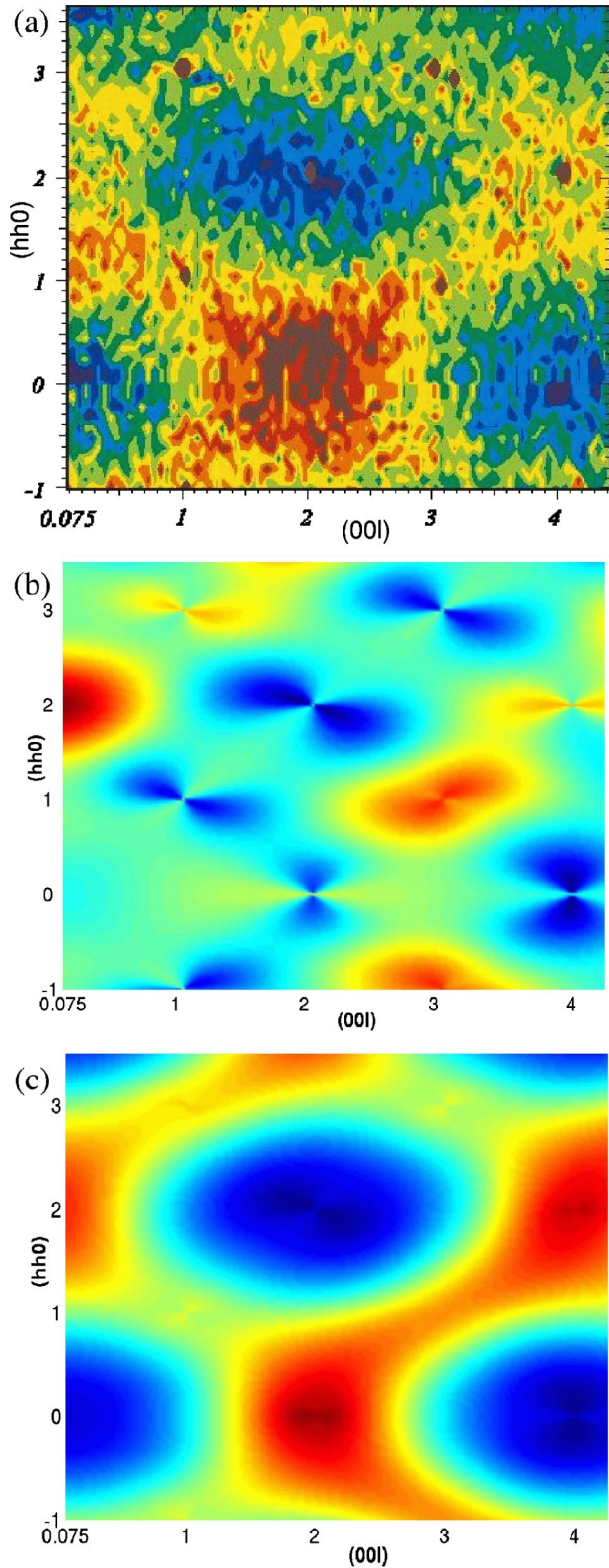
(a)

(b)

(c)

FIG. 1. (Color online) (a) Experimental elastic neutron scattering pattern of $Tb_2Ti_2O_7$ in the (h,h,l) plane of reciprocal space at $T=9$ K, from Ref. 16. Dark blue shows the lowest intensity level, red-brown the highest. (b) $S(\mathbf{Q})$ for the $\langle 111 \rangle$ Ising model at $T=9$ K. (c) $S(\mathbf{Q})$ for the doublet-doublet model at $T=9$ K. Note that magnetic form factor $|F(\mathbf{Q})|^2$ is divided out in both experimental and theoretical results.
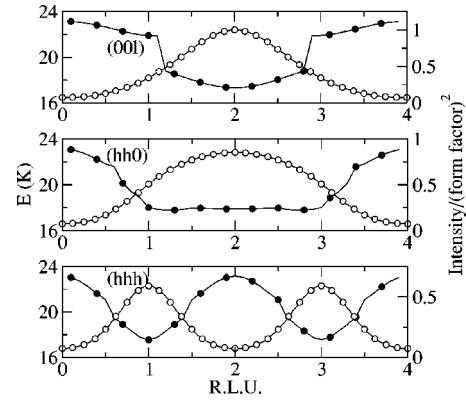

FIG. 2. The open symbols show the line scans of the $S(\mathbf{Q})$ for the three high-symmetry directions: from top to bottom, $(0,0,l)$, $(h,h,0)$, and (h,h,h). The filled symbols show the dispersion relation for the lowest-lying branch of magnetic excitations at $T=4$ K.

Single-ion excitations between the doublets are important in understanding the experimentally observed scattering pattern. These excitations originate in the first term of Eq. (2), where the anisotropy gap $\Delta = E_1 - E_0$ enters the formulation algebraically, instead of exponentially as in the elastic (second) term through the thermal occupation fraction. If the two-ion interaction, characterized by θ_{CW}, is comparable with Δ, then the effect of this term is large and part of the isotropic response is restored. By setting $\Delta \to \infty$ or the matrix element between two doublets to zero, this term is eliminated, and the scattering pattern is reduced to that of the $\langle 111 \rangle$ Ising model.[17] This explains why the $\langle 111 \rangle$ Ising model works so well in describing the spin correlations in spin ice materials,[8,10] since in these systems $\Delta \approx 200-300$ K (Refs. 20,21) and $\theta_{CW} \approx 0.5-2$ K,[8-10] so the effects of the excitations out of the ground-state doublet are negligible. To understand the different temperature dependencies of the dispersion for the three lowest-lying magnetic
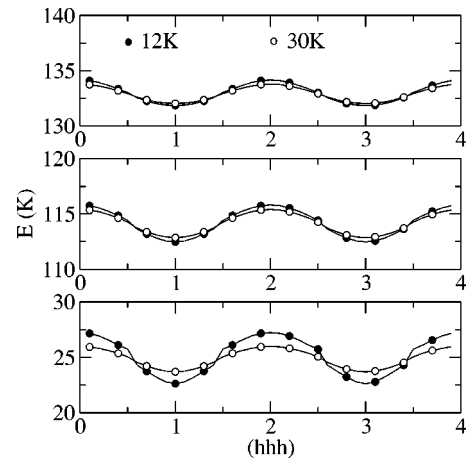

FIG. 3. The dispersion relations of the three lowest-lying magnetic excitations along the (h,h,h) direction at both 12 K and 30 K. The lowest band displays a more pronounced energy dispersion as temperature is lowered, in agreement with experimental observations.[16]

excitations, we inspect the thermal factor $n_{\nu\mu} = n_\nu - n_\mu$ in the first term of Eq. (2). For temperatures much lower than Δ, only the ground state doublet is populated, and this factor is almost the same for all three bands. When the temperature reaches a value $T \approx \Delta$, the first excited-state doublet begins to be populated, therefore reducing the factor $n_{01} = n_0 - n_1$, while those for the two higher levels remain essentially unchanged. This change in thermal occupation factor results in a large temperature dependence of the dispersion in the lowest band.

The low temperature ground state of our model in RPA is the noncollinear "all-in" or "all-out" $\mathbf{Q} = 0$ Néel state[10] with $T_c \approx 1.8$ K. The exact T_c value depends on the details of the crystal field wave functions. Surprisingly, this value is very close to T_c obtained recently in hydrostatic pressure measurements for pressure greater than 1 GPa.[27] The magnetic ground state doublet is a non-Kramers doublet, and the states are time conjugate of each other, so there exist no matrix elements between them,[28] indicating that any quantum fluc-

tuations causing spins to flip result from a higher-order virtual process via excited crystal-field levels.

In conclusion, with a simple level scheme and the RPA to include the excitations between the ground-state and the first excited-state doublets, we are able to describe quantitatively the experimentally observed paramagnetic neutron scattering pattern and the energy dispersion in $Tb_2Ti_2O_7$. Our results indicate that the crystal-field effects are important in this system due to the fact that the anisotropy gap and the two-ion interaction are comparable, and that some isotropy is present in the response. The ground state of our model, however, is still the all-in or all-out $\mathbf{Q} = 0$ Néel state[10] with $T_c \approx 1.8$ K, which is stable against the lowest order quantum fluctuations. These results indicate that a mechanism that may restore more isotropy, and thus increase the quantum fluctuations leading to the suppression of T_c, requires further detailed study.

---

*Electronic address: y2kao@uwaterloo.ca

[1] J. Villain, Z. Phys. B **33**, 31 (1979).

[2] J.N. Reimers, Phys. Rev. B **45**, 7287 (1992).

[3] R. Moessner and J.T. Chalker, Phys. Rev. Lett. **80**, 2929 (1998).

[4] A.P. Ramirez, B.S. Shastry, A. Hayashi, J.J. Krajewski, D.A. Huse, and R.J. Cava, Phys. Rev. Lett. **89**, 067202 (2002), and references therein.

[5] J.D.M. Champion, M.J. Harris, P.C.W. Holdsworth, A.S. Wills, G. Balakrishnan, S.T. Bramwell, E. Cizmar, T. Fennell, J.S. Gardner, J. Lago, D.F. McMorrow, M. Orendac, A. Orendacova, D. Mck. Paul, R.I. Smith, M.T.F. Telling, and A. Wildes, Phys. Rev. B **68**, 020401 (2003).

[6] A. Keren and J.S. Gardner, Phys. Rev. Lett. **87**, 177201 (2001), and references therein.

[7] M.J. Harris, S.T. Bramwell, D.F. McMorrow, T. Zeiske, and K.W. Godfrey, Phys. Rev. Lett. **79**, 2554 (1997).

[8] S.T. Bramwell, M.J. Harris, B.C. den Hertog, M.J.P. Gingras, J.S. Gardner, D.F. McMorrow, A.R. Wildes, A.L. Cornelius, J.D.M. Champion, R.G. Melko, and T. Fennell, Phys. Rev. Lett. **87**, 047205 (2001).

[9] A.P. Ramirez, A. Hayashi, R.J. Cava, R. Siddharthan, and B.S. Shastry, Nature (London) **399**, 333 (1999).

[10] B.C. den Hertog and M.J.P. Gingras, Phys. Rev. Lett. **84**, 3430 (2000).

[11] S.T. Bramwell and M.J.P. Gingras, Science **294**, 1495 (2002).

[12] S.T. Bramwell and M.J. Harris, J. Phys.: Condens. Matter **10**, L215 (1998).

[13] J.S. Gardner, S.R. Dunsiger, B.D. Gaulin, M.J.P. Gingras, J.E. Greedan, R.F. Kiefl, M.D. Lumsden, W.A. MacFarlane, N.P. Raju, J.E. Sonier, I. Swainson, and Z. Tun, Phys. Rev. Lett. **82**, 1012 (1999).

[14] M.J.P. Gingras, B.C. den Hertog, M. Faucher, J.S. Gardner, S.R. Dunsiger, L.J. Chang, B.D. Gaulin, N.P. Raju, and J.E. Greedan, Phys. Rev. B **62**, 6496 (2000).

[15] M.J.P. Gingras and B.C. den Hertog, Can. J. Phys. **79**, 1339 (2002).

[16] J.S. Gardner, B.D. Gaulin, A.J. Berlinsky, P. Waldron, S.R. Dunsiger, N.P. Raju, and J.E. Greedan, Phys. Rev. B **64**, 224416 (2001).

[17] M. Enjalran and M.J.P. Gingras, cond-mat/0307151 (unpublished).

[18] Y. Yasui, M. Kanada, M. Ito, H. Harashina, M. Sato, H. Okumura, K. Kakurai, and H. Kadowaki, J. Phys. Soc. Jpn. **71**, 599 (2002).

[19] R. Siddharthan, B.S. Shastry, A.P. Ramirez, A. Hayashi, R.J. Cava, and S. Rosenkranz, Phys. Rev. Lett. **83**, 1854 (1999).

[20] S. Rosenkranz, A.P. Ramirez, A. Hayashi, R.J. Cava, R. Siddharthan, and B.S. Shastry, J. Appl. Phys. **87**, 5914 (2000).

[21] S. Rosenkranz (private communications).

[22] M. Kanada, Y. Yasui, M. Ito, H. Harashina, M. Sato, H. Oakumura, and K. Kakurai, J. Phys. Soc. Jpn. **68**, 3802 (1999).

[23] R.P. Feynman, in *Progress in Low Temperature Physics*, edited by C.J. Gorter (Interscience, New York, 1955), Vol. 1.

[24] J. Jensen and A.R. Mackintosh, *Rare Earth Magnetism* (Clarendon Press, Oxford, 1991).

[25] $\mathcal{J}_1$ is estimated from $\theta_{CW}^{ex} \approx -14$ K, where the crystal field contribution is subtracted off from an effective paramanetic $\theta_{CW} \approx -19$ K (Ref. 14), and $J = 6$ for Tb^{3+}.

[26] M. Born and K. Huang, *Dynamical Theory of Crystal Lattices* (Oxford University Press, London, 1968), p. 228.

[27] I. Mirebeau, I.N. Goncharenko, P. Cadavez-Peres, S.T. Bramwell, M.J.P. Gingras, and J.S. Gardner, Nature (London) **420**, 54 (2002).

[28] A. Abragam and B. Bleaney, *Electron Paramagnetic Resonance of Transition Ions* (Clarendon, Oxford, 1970).